

# Estimating and scaling stream ecosystem metabolism along channels with heterogeneous substrate

Miki Hondzo,<sup>1\*</sup> Vaughan R. Voller,<sup>1</sup> Mark Morris,<sup>1</sup> Efi Foufoula-Georgiou,<sup>1</sup> Jacques Finlay,<sup>2</sup> Vamsi Ganti<sup>1</sup> and Mary E. Power<sup>3</sup>

<sup>1</sup> Department of Civil Engineering, Saint Anthony Falls Laboratory, University of Minnesota, Minneapolis, MN, USA

<sup>2</sup> Department of Ecology, Evolution, and Behavior, University of Minnesota, St. Paul, MN, USA

<sup>3</sup> Department of Integrative Biology, University of California Berkeley, Berkeley, CA, USA

## ABSTRACT

Measured diurnal curves of dissolved oxygen (DO) concentration have been used to estimate the gross primary production (GPP), ecosystem respiration (R), and net ecosystem production (NP) of aquatic communities. Open-system one-station and two-station methods have been employed to estimate the rate of NP, R, and GPP. We conducted field measurements in Minnehaha Creek, MN (44°56'N, 93°28'W), to quantify the spatial and temporal variabilities of DO concentrations and, consequently, evaluated the estimates of NP. Dimensionless analysis of DO mass balance revealed the dominance of local photosynthesis over respiration, advection, re-aeration, and dispersion along the studied reach. Two alternative estimation methods of stream metabolism provided similar estimates of NP with  $0.65 > k_a T_a > 0.17$  within the studied reach where  $k_a$  is the re-aeration rate and  $T_a$  is the water parcel average travel time. The spatial variability of DO change along the creek revealed an average length scale of 10 m over which DO exhibited significant autocorrelation. The autotrophic–heterotrophic balance, quantified by GPP to R ratio, scaled with local stream geomorphic and hydraulic conditions from diverse geographic areas, providing useful predictive relationships expressed in terms of easily measurable abiotic parameters. Copyright © 2013 John Wiley & Sons, Ltd.

KEY WORDS photosynthesis; respiration; gross primary production; fluid mechanics

Received 14 April 2013; Revised 8 April 2013; Accepted 8 April 2013

## INTRODUCTION

Aquatic ecosystem metabolism reflects many of the processes controlling organic matter processing and nutrient cycling and, thus, provides important information defining the trophic state of ecosystems (Dodds and Cole, 2007). *In situ* measurement of dissolved oxygen (DO) concentration has been used to quantify the metabolism of flowing water communities (Odum, 1956; Hornberger *et al.*, 1977; Erdman, 1979; Mulholland *et al.*, 2001; Roberts *et al.*, 2007; Loperfido *et al.*, 2009; Reichert *et al.*, 2009; Bernot *et al.*, 2010; Demars *et al.*, 2011; Hunt *et al.*, 2012). A diurnal change in DO concentration is determined by photosynthetic primary production, respiration, and gas exchange with the atmosphere (Bott, 2006). Algae and other aquatic plants are responsible for gross primary production (GPP), whereas total respiration (R) measures the rates of respiration by aquatic plants, algae, fish, invertebrates, and microbes. Open-system single-station and two-station methods have been used to estimate the whole-ecosystem

rate of GPP and R in flowing waters (Odum, 1956; Hall, 1972; Erdman, 1979; Bott, 2006; McCutchan and Lewis, 2006; Reichert *et al.*, 2009). The single-station method assumes that a point measurement reflects averaged conditions over a longer, relatively homogeneous reach, over a time interval in which oxygen is not influenced by fluctuations in oxygen concentrations in discharge arriving from upstream. The two-station method uses DO concentration measurements at upstream and downstream stations along the stream. The DO concentration in the stream is determined by GPP, R, and the atmospheric gas exchange along the reach, and in some cases, groundwater inputs.

A major constraint on using stream ecosystem metabolism as a management or restoration indicator is the low temporal and spatial frequencies at which metabolism measurements are conducted. Although four scales of temporal variability in stream metabolism (seasonal, diurnal, episodic storm-related, interannual) have been distinguished (Roberts *et al.*, 2007), limited information on systematic spatial variability through stream reaches is available. Reichert *et al.* (2009) has explicitly addressed the effect of large-scale heterogeneities (e.g. changes in land surface cover, topography, stream morphology) on estimates of stream metabolism from oxygen measurements.

\*Correspondence to: Miki Hondzo, Department of Civil Engineering, University of Minnesota, St. Anthony Falls Laboratory, 2nd Third Ave SE, Minneapolis, MN 55414-2196, USA. E-mail: mhondzo@umn.edu

McTammany *et al.* (2003) reported significant variabilities in GPP and R at four sites along a 37-km segment of the Little Tennessee River, NC. Spatial heterogeneity in algal biomass attached to sediments (periphyton) has been reported from local cross-sectional scale to the reach scale of several kilometres (Biggs *et al.*, 2005; Barnes *et al.*, 2007; Warnars *et al.*, 2007; Hunt *et al.*, 2012). Spatial variability of biogeochemical activity in stream sediments creates 'hot spots and hot moments' of oxygen and nitrate reduction along streams (McClain *et al.*, 2003; Fisher *et al.*, 2004; O'Connor *et al.*, 2006; O'Connor and Hondzo, 2007; Knapp *et al.*, 2009). Finlay (2011) found strong spatial patterns in GPP in stream networks largely related to channel width and light availability, whereas R was less spatially variable. Given the spatial heterogeneities of gross primary producers and respiring bacteria, what is a characteristic spatial scale in stream ecosystem metabolism? How representative are stream metabolism estimates (Bott, 2006) by various procedures for the one-station and two-station methods?

The objective of this study was to (1) examine small scale spatial heterogeneities of DO concentrations in a stream with a productive aquatic macrophyte assemblage; (2) estimate stream metabolism at the reach scale by one-station and two-stations methods; and (3) investigate a scaling relationship between stream ecosystem metabolism and standard abiotic variables from our data and data reported in other geographical areas. The proposed scaling relationship arising from this work could potentially be used to predict stream network metabolism from local geomorphic and hydraulic conditions.

## MATERIALS AND METHODS

### Study site

Field measurements were conducted in Minnehaha Creek, MN, at base flow over diurnal time scales from 8 June to 19 June 2007. The creek is a tributary of the Mississippi River, located in the Minnehaha watershed with a watershed area of 100 km<sup>2</sup> upstream of the measuring reach. Field measurements were conducted at the headwaters of Minnehaha Creek, whereas the discharge in the stream is controlled by a sluice gate at the outfall of Lake Minnetonka. The terrain surrounding the creek at the measuring reach is open, flat marsh, and wetland (Figure 1). The stream has simple geometry, nearly constant discharge, and even exposure to sunlight. The stream bed is largely covered by common macrophytes (*Potamogeton illinoensis*, *Ceratophyllum demersum*, *Myriophyllum sibiricum*) and periphyton.

### Equipment

Dissolved oxygen, stream temperature, conductivity, and pH measurements were collected using a Hydrolab Datasonde 5x multiparameter platform with Luminescent

Dissolved Oxygen sensor (Hach Company, Loveland, CO, USA). The sondes were placed at the designated sampling sites and simultaneously recorded the water quality variables in the creek (Figure 1). Prior to deployment, the multiprobes were calibrated in the laboratory under identical temperature and DO concentrations. The water quality variables described previously were sampled continuously at 1-min intervals from 9 June to 12 June 2007. Flow and sediment topography measurements were made using a StreamPro acoustic-Doppler current profiler (RD Instruments, Poway, CA, USA). Point velocity profiles were recorded at 1-s sampling intervals using an acoustic-Doppler velocimeter (Sontek YSI Inc., San Diego, CA, USA).

A canoe equipped with a DO concentration microsensors (OX-50 standard with 90% response time less than 5 s, Unisense, Denmark), Hydrolab Datasonde, sonar bed-topography profiler, and the acoustic-Doppler velocimeter was employed to measure the spatial variability of DO, temperature, and velocity along the measuring reach. All sensors were submersed about 10 cm below the water surface and placed in the bow of the boat, outside the influence of paddle activity to minimize the influence of canoe movement on the measuring variables. DO was sampled at 5-s intervals, and the data was stored in a data logger. Several longitudinal profiles were conducted along the measuring reach (from site 0 to site 4) with the canoe on June 11, 15, and 19. The canoe was generally positioned at a mid-distance between the banks and followed the main stream direction along the creek.

### Dissolved oxygen balance

A mass balance for DO concentration in a stream can be written as

$$\frac{\partial C}{\partial t} + U \frac{\partial C}{\partial x} = \frac{1}{A} \frac{\partial}{\partial x} \left( EA \frac{\partial C}{\partial x} \right) - \frac{C}{A} \frac{\partial}{\partial x} \left( \frac{\partial Q}{\partial x} + \frac{\partial A}{\partial t} \right) + k_a(C_s - C) + GPP - R \quad (1)$$

where  $C$  is the cross-sectional-averaged DO concentration,  $t$  is time,  $U$  is the discharge velocity in the  $x$  direction,  $A$  is the stream cross-sectional area,  $Q$  is the total discharge,  $E$  is the longitudinal dispersion coefficient,  $k_a$  is the re-aeration rate, and  $C_s$  is the DO saturation concentration. For a stream with insignificant dispersive transport, discharge variability along the stream, and variability in cross-sectional area over time, Equation (1) simplifies to

$$\frac{\partial C}{\partial t} + U \frac{\partial C}{\partial x} = k_a(C_s - C) + GPP - R \quad (2)$$

To compare the magnitude of different terms in Equation (2), we define DO deficit as  $D = C_s - C$ , and scale the variables by the following



Figure 1. Minnehaha Creek, MN, with sampling sites 0–4 along the creek. Water quality sensors fixed at measuring sites quantified temperature and dissolved oxygen variabilities  $\frac{\partial C}{\partial t}|_{\text{Site } 1-4} = f(t)$ . In the canoe fixed sensors, water temperature and dissolved oxygen variabilities were quantified  $\frac{dC}{dt} = f(\tilde{x}, t)$ .

$$\begin{aligned} \hat{D} &= \frac{D}{D_o} \tau = \frac{t}{T} & \hat{u} &= \frac{U}{U_o} \\ \xi &= \frac{x}{L} & \hat{k}_a &= \frac{k_a}{k_{a0}} & \hat{GPP} &= \frac{GPP}{GPP_o} & \hat{R} &= \frac{R}{R_o} \end{aligned} \quad (3)$$

where  $D_o$ ,  $T$ ,  $U_o$ ,  $L$ ,  $k_{a0}$ ,  $GPP_o$ , and  $R_o$  are characteristic scales with identical dimensions as the corresponding variables. Therefore, the scaled variables in Equation (3) are dimensionless. Under the specific case that the saturation concentration is a constant, we can combine Equations (1) and (3) into a single equation in terms of the DO deficit.

$$\frac{\partial \hat{D}}{\partial \tau} + \tau_a \hat{u} \frac{\partial \hat{D}}{\partial \xi} = \tau_D \frac{\partial \hat{D}^2}{\partial \xi^2} - \tau_{ar} \hat{D} - \tau_{GPP} \hat{GPP} + \tau_R \hat{R} \quad (4)$$

Although the assumption of a constant  $C_s$  is limited and will not be used at later points in this work, here, it allows us to clearly define the important time scales of the process, in particular with reference to Equation (4), we have the following nondimensional time scales

$$\begin{aligned} \tau_a &= \frac{U_o T}{L} & \tau_D &= \frac{T E}{L^2} & \tau_{ar} &= \frac{T}{1/k_{a0}} \\ \tau_{GPP} &= \frac{T}{D_o / GPP_o} & \tau_R &= \frac{1}{D_o / R_o} \end{aligned} \quad (5)$$

The nondimensional time scales in Equation (5) represent advection, longitudinal dispersion, diffusion across the air–water interface, photosynthesis, and respiration processes, respectively. The corresponding dimensional time scales are  $T_a = L/U_o$ ,  $T_D = L^2/E$ ,  $T_{ar} = 1/k_{a0}$ ,  $T_{GPP} = D_o/GPP_o$ , and  $T_R = D_o/R_o$ . The estimates of time scales of the processes involved are instrumental to identify the dominant processes in a mass balance for DO concentration in a stream. The longitudinal dispersion coefficient can be estimated as proposed by Fischer (1975) by  $E = 0.011 \frac{U_o^2 B^2}{H u_*}$  where  $U_o$  is the stream discharge velocity,  $B$  is the wetted stream width,  $H$  is the cross-

sectional averaged depth,  $u_* = \sqrt{gHS}$  is the bed shear-stress velocity, and  $S$  is the mean stream slope.

Equation (2) is a starting point for developing estimates of metabolism in streams. Typically, these estimators are casted as one-station and two-station methods. One-station methods use DO measurements at a single location in the stream, and for specified  $k_a$ , provide an estimate of  $GPP$  and  $R$ . The method is applicable in long homogenous reaches where  $T_a k_a > 3$  (Chapra and Di Torro, 1991; Reichert *et al.*, 2009), a condition that simplifies Equation (2) to

$$\begin{aligned} \frac{\partial C}{\partial t}|_{x=\text{fixed}} &= k_a(C_s - C) + GPP - R \\ &= k_a(C_s - C) + NP \end{aligned} \quad (6)$$

where  $NP$  is the net DO production in the reach as a result of  $GPP$  and  $R$  (net ecosystem production per water volume of the stream). The term  $\partial C/\partial t|_{x=\text{fixed}}$  is evaluated from the DO measurements at a fixed downstream location in the stream.

In contrast, the two-station methods use DO concentration measurements at two fixed stations along the stream, and for specified  $k_a$ , provide an estimate of  $NP$ ,  $R$ , and  $GPP$  (Bott, 2006). The method is also based on Equation (2), the same starting point as the one-station method; however, the change in DO concentration is referenced with respect to a moving reference frame (e.g. Hornberger and Kelly, 1975; McCutchan and Lewis, 2006) which allows this method to account for the total rate of change of DO along  $x$ -distance of the stream defined as  $\frac{dC}{dt} = \frac{\partial C}{\partial t} + U \frac{\partial C}{\partial x}$ . Thus, the resulting transport equation is

$$\frac{dC}{dt} = k_a(C_s - C) + GPP - R = k_a(C_s - C) + NP \quad (7)$$

The fundamental assumption in using Equation (7) is the existence of a characteristic velocity with which successive parcels of water are advected between the two measuring stations. In this way, the estimation of  $dC/dt$  depends on how the DO concentration in a given parcel changes over

the travel time ( $T_a$ ). The operation of the two-station method rests in evaluating the temporal average  $\frac{1}{T_a} \int_0^{t+T_a} k_a(C_s - C)dt'$ , where  $T_a$  is the travel time of a water parcel between the upstream and downstream stations. The most frequently employed method in practice, summarized by Bott (2006), estimates this quantity with a trapezoidal rule that averages the values at the upstream station at time ' $t$ ' and the downstream station at time ' $t+T_a$ '. In an alternative approach, Reichert *et al.* (2009) uses an analytical solution of Equation (2).

Insight in how the DO concentration changes in successive parcels of water could be assessed by measuring the DO concentration profile along the stream. A reasonable estimate can be obtained by scanning DO concentrations at a rate faster than the characteristic travel time. From this data, a convenient measure of the extent of the region over which DO concentrations are appreciably correlated can be estimated by the integral length scale (e.g. Kundu, 1990, p. 424; Bewley *et al.*, 2012)

$$L = \int_0^{\infty} \rho(\tilde{x}') d\tilde{x}' \quad (8)$$

where  $\rho(\tilde{x}')$  is the autocorrelation function of DO concentration, and  $\tilde{x}'$  is the distance lag along the stream (e.g. distance lag between two points is  $\tilde{x}' = \tilde{x}_2 - \tilde{x}_1$ ). The integral length scale could be interpreted as a measure of the 'memory' of the DO concentration change along the stream.

Dissolved oxygen flux at the air–water interface, i.e. re-aeration rate, was determined at one site using the volatile tracer method (Bott, 2006), where exchange of oxygen between the stream reach and the atmosphere is estimated from the downstream loss of an introduced gas (in this case, propane). Propane was added at a constant rate at four points spread across the stream channel as through microbubble injections using aquarium air

stones 250 m upstream of site 3 (Figure 1). After 3 h of propane injection to allow time for adequate mixing (based on  $\gg 3$  times the mean water travel time estimated from flow and channel geometry), four propane samples were collected at each of four stations along a longitudinal transect 200, 250, 300, and 350 m downstream of the propane injection point. These samples were collected into syringes without exposure to the atmosphere and transported back to the lab on ice. The following day, propane concentration was determined by equilibrating water with laboratory air and injecting a headspace sample into a Shimadzu gas chromatograph (Model 14) equipped with a flame ionization detector. Propane concentration exchange coefficients were estimated using changes in propane with distance according to a model based on the rate of propane loss (Bott, 2006). Propane exchange coefficients were converted to oxygen exchange coefficients by multiplying by 1.39. We assumed that effects of groundwater dilution of propane along the reach were minimal because of the relatively large stream flow volume, the lack of springs, and the wide, flat valley setting of the site.

## RESULTS

### Fluid flow

The cross-sectional Reynolds number was larger than 4000 at all measuring stations indicating that measurements were conducted in a turbulent flow (Table I). The ratio of inertial to gravitational forces, Froude number, indicated subcritical fluid-flow conditions in the channel. The reach mean travel time scale,  $T_a = \frac{L}{U_0} = \frac{2089\text{m}}{0.079\text{ m/s}}$ , of about 7.3 h was significantly smaller than the dispersive time scale,  $T_D = \frac{L^2}{E} = \frac{2089^2\text{ m}^2}{0.92\text{ m}^2/\text{s}}$ , of 1317 h. The ratio between these two time scales, defined by the Peclet number  $Pe = \frac{T_D}{T_a}$ , indicates  $Pe = 160$  and, therefore, advection dominated ( $Pe \gg 1$ ) fluid-flow transport.

Table I. Hydraulic and geometric data for study reaches. An average slope of the reach is  $S = 0.00025$ .

	Distance along the creek	Cross-sectional area	Wetted stream width	Cross-sectional averaged depth	Discharge velocity	Froude number	Reynolds number
	$x$ (m)	$A$ (m <sup>2</sup> )	$B$ (m)	$H$ (m)	$U$ (m/s)	$\frac{U}{\sqrt{gH}}$ Fr (–)	$\frac{UH}{\nu}$ Re (–)
Site							
0	0	24.8	36	0.69	0.043	0.017	29 700
1	607	18.7	31.0	0.61	0.057	0.023	34 800
2	1048	16.5	27.0	0.61	0.064	0.026	39 000
3	1709	9.8	19.5	0.51	0.109	0.049	55 600
4	2089	8.9	23.4	0.38	0.120	0.062	45 600
Reach	—	—	—	—	—	—	—
Average	—	15.74	27.38	0.56	0.079	0.028	39 460

Dissolved oxygen

The DO time series for sampling sites 1–4 depict the typical diurnal patterns with maximum DO concentration within 2 h prior to sunset (11 Jun 2007; 21:00 h) and minimum within 1 h after the sunrise (11 June 2007; 5:26 h) (Figure 2). The simultaneous measurements display variability in the magnitude and timing of maximal and minimal DO concentrations. The maximal simultaneous DO difference among sites was 2.1 mg/l, and the minimal difference was 1.6 mg/l. The largest time lag among the maximal concentrations was up to 2.5 h and 1 h for the minimal concentrations. The diurnal patterns in the DO saturation deficit,  $D = DO_s - DO$ , suggest an autotroph-dominated environment, where DO concentrations were above saturation, and consequently, the deficit was negative for significant time periods during the measurements (Figure 2).

The objective of the canoe-based oxygen profile was to measure inherent spatial and temporal variability of DO along the study reach. The spatial heterogeneity in DO concentration along the creek is depicted in Figure 3. Two DO sensors fixed on the canoe-sampled DO concentrations along the study reach. The canoe travel time, displayed on the  $x$ -axis, was on average five times faster than the stream mean travel time among the sampling stations. The velocity of the canoe was restricted by the DO sensor response time. The transects by canoe were conducted at different days and times during the measurements. DO changed appreciably in magnitude along the stream (Figure 3). The spatial heterogeneity of the total change of DO along the stream measured within the canoe reference frame,  $d\tilde{C}/dt$ , displays a variety of positive and negative slopes within the consecutive reaches and along the entire reach.

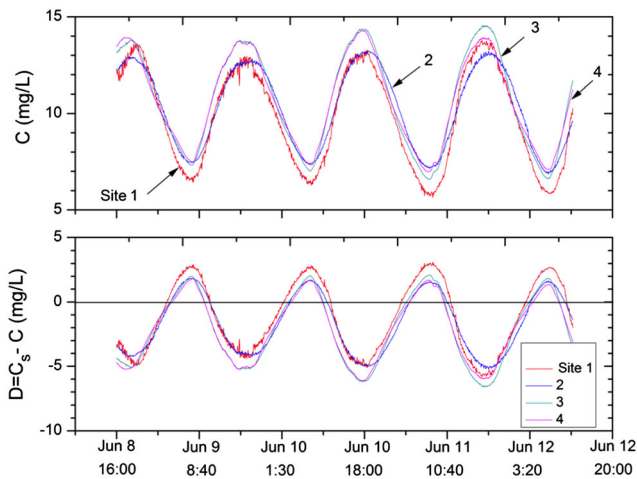


Figure 2. Dissolved oxygen concentration ( $C$ ) and DO deficit ( $D = C_s - C$ ) time series measured at 1-min interval at sampling sites 1–4. During the measurements, the saturated DO concentration of  $C_s$  ranged from 7.9 to 8.4 mg/l.

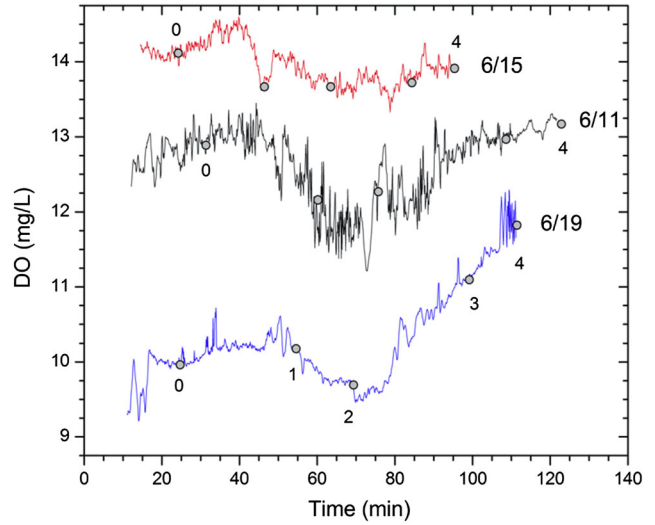


Figure 3. Dissolved oxygen concentration measured at 5-s interval from the canoe along the stream. The dots with numbers indicate sampling sites with fixed DO sensors.

The length scale over which significant correlation of the total change of DO along the stream existed,  $d\tilde{C}/dt$ , was quantified by integrating the autocorrelation function, Equation (8), of  $d\tilde{C}/dt$ . We analysed the stationary increments of  $d\tilde{C}/dt$  for different lag distances along the stream. The autocorrelation function generally decreased rapidly to its first zero-crossing after which it remained negative and oscillated around zero (Figure 4). High correlation with several data points was observed prior to the zero-crossing, which indicated the appropriate sampling frequency of DO sensors. The integrated autocorrelation function provided the integral length scale,  $L$ , that is, the

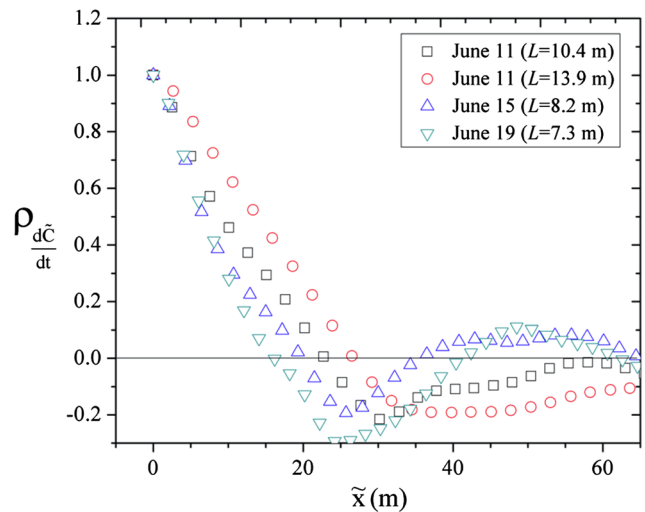


Figure 4. Autocorrelation functions for the longitudinal concentration gradients. The transects were conducted by the canoe on June 11 (12:15 h; square symbol), June 11 (17:00 h), June 15 (14:45 h), and June 19 (11:00 h).

measure of the correlation distance between the  $d\tilde{C}/dt$  of two sampling points along the stream. Usually, the portion of the area under the  $\rho(\tilde{x})$  that spans from  $\tilde{x}=0$  to  $\tilde{x}=l_a$ , where  $l_a$  is the first value of  $\tilde{x}$  which corresponds to  $\rho(\tilde{x})=0$  is considered in the integral length scale estimation (Hassan *et al.*, 2005). The integral length scale ranged from  $L=7.3$  to 13.9 m distance along the stream (Figure 4). An alternative method is to integrate  $\rho(\tilde{x})$  from  $\tilde{x}=0$  to  $\tilde{x}=l_b$ , where  $l_b$  is the value of  $\tilde{x}$  which corresponds to a minimum value of  $\rho(\tilde{x})$ . The alternative method provided similar estimates of the integral length scale from  $L=6.6$  to 11.0 m. Therefore, the largest distance over which the total change in DO was correlated was up to  $L=13.9$  m. An average integral length scale was on the order of a half-average width of the Minnehaha Creek along the measuring sites (Table I). The time required to advect an average integral length by the creek discharge velocity in the creek was on the order of  $\bar{t}=L/U_o=10.6/0.079=134$  s. This time was twice as long as the sampling time interval at the fixed measuring sites along the Minnehaha Creek, ensuring that our measurements were of adequate temporal resolution.

Oxygen flux at the air–water interface was estimated from the propane concentration measurements along the creek. The decrease of propane concentration with distance downstream was explained by the functional relationship suggested by Young and Huryn (1998) with the estimated  $r^2=0.94$  for a regression analyses of propane concentration data and distance. The air–water exchange rate of oxygen, estimated directly from the propane concentrations, was  $k_a=3.39$  (1/day). A large number of empirical equations have been reported in the literature to relate the re-aeration rate with stream hydraulic characteristics (e.g. Jain and Jha, 2005). Our field estimate of  $k_a$  was closely predicted by the relationships proposed by O'Connor and Dobbins (1958),  $k_a=3.93 U^{0.5}/H^{1.5}=3.56$  (1/day) (Table I, Site 3), and the expression proposed by Chu and Jirka (2003),  $k_a=\frac{1.792}{H}\left(\frac{g}{H}\right)^{0.336}=\frac{1.792}{H}\left(\frac{g}{H}\right)^{0.336}$  (1/day). The O'Connor and Dobbins relationship was used in the estimation of  $GPP$  and  $R$  from DO measurements at other sites along the stream.

#### Net ecosystem production

Daily  $GPP$ ,  $R$ , and  $NP$  rates were estimated from the diurnal DO and temperature data (Figure 2). Two alternative estimators, described in methods section, were employed including the most frequently used approach or the state of practice approach, summarized by Bott (2006), and the approach suggested by Reichert *et al.* (2009; Equation 26 for the two-station method and Equation 27 for the one-station method). Because the field measurements were conducted over three consecutive days, the diurnal estimates of  $NP$  were estimated for each daily cycle separately, and the data were averaged over the measure-

ment period (Table II). All methods indicated daily- and reach-averaged  $NP\sim 2$  or above indicating net DO production and the dominance of local photosynthesis in the stream. The magnitudes of  $NP$  were within the reported range of ecosystem metabolism (e.g. Mulholland *et al.*, 2001; Roberts *et al.*, 2007). The estimates of  $NP$  from the one-station method were approximately half the estimates from the two-station method (Table II). The studied reach is not long enough ( $T_a k_a=0.91$ ) to be considered as a long homogenous reach, where  $T_a k_a>3$ . However, both one-station methods (Bott 2006; Reichert *et al.*, 2009) provided comparable estimates of  $NP$ . The two-station methods provided similar estimates of  $NP$  along the studied reach (Table II). The two-station method proposed by Reichert *et al.* (2009), assumes that the length of the study reach of  $T_a k_a$  must be  $>0.4$  in order to accurately estimate  $NP$ . Although reach 1–2 ( $T_a k_a=0.17$ ), 2–3 (0.24) and 3–4 (0.17) had shorter length than this suggested criterion, the estimates of  $NP$  were consistent in comparison to the two-station method proposed by Bott (2006). Reaches with longer length  $T_a k_a>0.4$  (reach 1–3, 2–4, and 1–4) provided similar estimates of  $NP$  along the studied reach by both methods. The estimation of  $R$ , during darkness, and extrapolation during the daylight hours were conducted as suggested by Bott (2006) and Reichert *et al.* (2009). The reach average estimate of  $GPP$  was  $9.59$  ( $\text{g O}_2/\text{m}^2/\text{day}$ ) and  $R$  was  $3.90$  ( $\text{g O}_2/\text{m}^2/\text{day}$ ).

#### Characteristic temporal scales

The preceding analysis provided variables that can be used to gain insight on the various hydraulic and biological processes that determine DO variability in the stream. The

Table II. Daily average fluxes of net dissolved oxygen production (NP) as a result of gross primary production (GPP) and total respiration (R) estimated by the one-station and two-station methods in Minnehaha Creek, from 8 June to 12 June 2007.

Estimation method	NP* (GPP – R) ( $\text{g O}_2/\text{m}^2/\text{day}$ )	NP** (GPP – R) ( $\text{g O}_2/\text{m}^2/\text{day}$ )
One-station		
1	2.00	1.65
2	2.76	2.63
3	3.47	4.54
4	4.64	5.53
Reach average	3.22	3.59
Two-station		
Reach 1–2 ( $\tau_{ar}=T_a k_a=0.17$ )	6.82	6.68
Reach 2–3 ( $\tau_{ar}=0.24$ )	5.25	5.28
Reach 3–4 ( $\tau_{ar}=0.17$ )	5.50	5.16
Reach 1–4 average	5.85	5.71
Reach 1–3 ( $\tau_{ar}=0.41$ )	5.97	6.36
Reach 2–4 ( $\tau_{ar}=0.45$ )	4.93	4.99
Reach 1–4 ( $\tau_{ar}=0.65$ )	5.30	5.69

\*Bott (2006); \*\*Reichert *et al.* (2009)

estimated dimensional time scales, specified by Equation (5) are advection  $T_a = LU_o = 7.38$  h, dispersion  $T_D = L^2/E = 1317.61$  h, aeration  $T_{ar} = 1/k_{ao} = 8.08$  h, photosynthesis  $T_{GPP} = D_o/GPP_o = 1.98$  h, and respiration  $T_R = D_o/R_o = 4.87$  h (where  $D_o = 1.62$  g/m<sup>3</sup>,  $GPP_o = 19.37$  g/m<sup>3</sup>/day, and  $R_o = 7.88$  g/m<sup>3</sup>/day). The magnitude of time scales implies  $T_{GPP} < T_R < T_a \sim T_{ar} < T_D$ , that is, the dominance and importance of photosynthesis over respiration, advection, aeration and transport by dispersion along the studied reach.

*Scaling ecosystem metabolism*

Identification of a power law relation between metabolic processes and abiotic drivers is a challenging topic. Because abiotic stream variables, including geomorphology and hydraulics, are easier to estimate than biological variables, such scaling relationships could be instrumental for *GPP* and *R* prediction over a range of scales. Odum (1956) proposed the ratio of *GPP/R* to classify aquatic environments according to their predominantly autotrophic (*GPP/R* > 1) or heterotrophic (*GPP/R* < 1) characteristics. Warnars *et al.* (2007) explored the dimensionless ratio of *GPP/R* as influenced by parameters, expressed as dimensionless numbers, that integrate local stream geomorphology and hydraulics. The estimated *GPP* and *R* values, based on the one-station method, of this study and a variety of other studies conducted across a range of geomorphic and climatic conditions are provided in Figure 5. *GPP* to *R* ratios followed a functional dependence

$$\frac{GPP}{R} = 0.02 \left(\frac{B}{H}\right)^{6/5} \left(\frac{U}{u_*}\right)^{2/5} \quad (9)$$

The observed functional dependence (Equation 9 and Figure 5) implies that stream geomorphology exerts a significant control on stream metabolism. In forested watersheds, stream width can be interpreted as a surrogate for photosynthetically active radiation exposure (Finlay *et al.*, 2011), and stream depth represents the attenuation of photosynthetically active radiation. The ratio of  $u_*/U$  could be interpreted by a bed resistance coefficient,  $C_f \sim u_*/U$ , whereas increased bed resistance promotes larger momentum flux at the bed and consequently initiates the movement of fine bed sediments and effectively reduces the *GPP/R* ratio.

DISCUSSION

In this work, two alternative two-station methods have been tested. One, which we term state of the practice approach, was outlined in detail by Bott (2006), and the other, more recent approach, Reichert *et al.*, (2009), is based

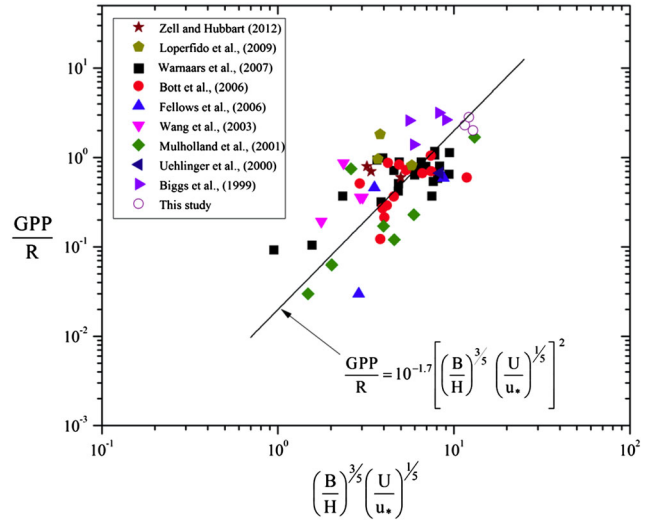


Figure 5. Ecosystem functional classification according to the total metabolism of autotrophic (*GPP*) and heterotrophic (*R*) communities versus stream geomorphology and hydraulic conditions.

on an analytical solution of Equation (2). For the field data used in this work, we see that the estimates of *NP* from both methods are very similar (Table II). It is instructive to explain why, under our field conditions, these results should be similar. Two-station methods are arrived at under the assumption that a parcel of fluid will move intact through a reach of length *L* with a characteristic velocity  $U = L/T_a$ . After a temporal averaging over the travel time, Equation (7) can be rearranged and written as

$$\langle NP \rangle = \left\langle \frac{dC}{dt} \right\rangle - k_a \langle (C_s - C) \rangle \quad (10)$$

where the notation  $\langle \bullet \rangle = \frac{1}{T_a} \int \bullet dt'$ . It is assumed (with no real loss of generality) that the aeration coefficient  $k_a$  is constant in the reach, and *NP* represents the averaged net production rate of the reach over the travel time. Without any loss of accuracy we can then write Equation (10) in terms of values of concentration at the upstream (up) and downstream (dn) stations, i.e.

$$\langle NP \rangle = \frac{C^{dn}(t + T_a) - C^{up}(t)}{T_a} - k_a \langle (C_s - C) \rangle \quad (11)$$

This equation provides an exact accounting of the average *NP* in the reach over the given travel time. To make a calculation, however, we need to approximate the last term on the right-hand side of Equation (11). In the basic two-station method (Bott, 2006), a trapezoidal integration rule is used

$$\begin{aligned}
k_a \langle (C_s - C) \rangle &= \frac{k_a}{T_a} \int_t^{t+T_a} (C_s - C) dt' \\
&\approx k_a \frac{(C^{\text{dn}}(t+T_a) + C^{\text{up}}(t))}{2} - k_a \frac{(C_s(t+T_a) + C_s(t))}{2}
\end{aligned} \quad (12)$$

an approximation that will be reasonable if the change in the DO deficit  $D = C_s - C$  with time is linear or small. In contrast to the basic two-point method, the recent alternative scheme of Reichert *et al.* (2009) does not start from the Lagrangian form in Equation (7) but rather develops an approach based on an analytical solution in the Eulerian framework of Equation (2). Nevertheless, the final working form, Equation (26) in Reichert *et al.* (2009), can be readily rearranged to fit the form in Equation (11). Such a rearrangement gives the following representation for the last term on the right of Equation (11)

$$k_a \langle (C_s - C) \rangle \approx k_a \left[ \frac{[k_a T_a - (1 - \alpha)] C^{\text{dn}}(t + T_a) + [(1 - \alpha) - \alpha k_a T_a] C^{\text{up}}(t)}{k_a T_a (1 - \alpha)} \right] - k_a C_s(t^*) \quad (13)$$

where  $t^* = t + T_a \left[ \frac{1}{1-\alpha} - \frac{1}{k_a T_a} \right]$  and  $\alpha = \exp(-k_a T_a)$ . For values of  $k_a T_a \sim 0.5$  and below, where it is reasonable to make the approximation  $k_a T_a \approx 2(1 - \alpha)/(1 + \alpha)$ , it can be shown, with some algebra, that the right-hand side of Equation (13) approximates the right-hand side of Equation (12). For example, if  $k_a T_a = 0.5$  (within the range of values in Table II), the right-hand side of Equation (13) is

$$\begin{aligned}
k_a \langle (C_s - C) \rangle &\approx k_a [0.54 C^{\text{dn}}(t + T_a) + 0.46 C^{\text{up}}(t)] \\
&\quad - k_a C_s(t + 0.54 T_a)
\end{aligned} \quad (14)$$

an approximation, that under reasonable circumstances, should be close to that used in the basic two-station approximation of Equation (12). Clearly, however, with larger values of  $k_a T_a$ , beyond what we are seeing in our field setting, we would expect more difference between the basic Equation (12) and the modified Equation (13) approximations.

We point out that in the Lagrangian (two-station) estimation method,  $dC/dt$  is computed at each sampling time by the DO concentration differences between the downstream and upstream measuring stations and dividing by the time of the flow ( $\frac{dC}{dt} \sim \frac{\Delta C}{\Delta x} U$ ). Our data suggest that the approximation of  $\langle \frac{dC}{dt} \rangle \sim U$  is not violated over the average integral length scale of up to  $L = 10$  m along the creek. The scale-dependence of the sort shown in  $\langle \frac{dC}{dt} \rangle \sim U$  might be relaxed and potentially applied over longer spatial scales by using fractional derivatives, i.e.,  $\frac{d^m C}{dt^m} \sim u'$  where  $u'$

is some reference velocity for the water parcel (Podlubny, 1999), and the order of fractional derivative 'n' should be estimated from data ( $1 > n > 0$ ). An equivalent way of seeing the previous fractional differentiation is by taking the derivative of a 'smoothed' version of  $C(t)$ , i.e.  $\frac{d}{dt} (I_t^\gamma C) \sim u'$ , where  $I_t^\gamma(\cdot)$  denotes the fractional integration of a time series to an order of  $0 < \gamma \leq 1$ , and  $\gamma = 1 - n$ . It is beyond the scope of this paper to develop a proper Lagrangian estimator of  $GPP$ ,  $R$ , and  $NP$  that is consistent with the proposed scale-dependence. Such an estimator requires specific field measurements and will be the subject of a future study.

Demars *et al.* (2011) proposed an interesting intuitive method that accounts for spatial heterogeneity in estimation of stream metabolism along a reach scale. The proposed method advocates averaging of observed DO concentrations along the reach and consequently employs a variant of one-station method to the averaged DO concentration time series in the estimation of stream metabolism.

Although the method could have a challenging mathematical justification considering imbedded nonlinear relationships among  $C_s$ ,  $k_a$ , and local stream physical variables, an open question is how many DO sampling sondes are required to deploy in order to estimate a reach average metabolism. Reichert *et al.* (2009) proposed the estimation of stream metabolism from DO measurements in the presence of large-scale heterogeneities including changes in land surface cover and corresponding DO production due to changes in light intensity and variabilities in stream geomorphology. Considering the large-scale heterogeneities, a local linear approximation over periods of hours appears to be adequate. In Minnehaha Creek with stream bed covered by macrophytes, the proposed method provided consistent estimates of  $NP$  along the stream with  $0.65 > T_a k_a > 0.17$ .

The autotrophic–heterotrophic balance, quantified by  $GPP$  to  $R$  ratio, was empirically predictable from local stream geomorphic and hydraulic conditions (Figure 5). Stream aspect ratio ( $B/H$ ) emerged as an important control of autotrophic–heterotrophic balance in streams (Vannote *et al.*, 1980; Barnes *et al.*, 2007; Warnars *et al.*, 2007). The corresponding hydraulic conditions, quantified by  $U/u_*$  ratio, contributed to the modulation of autotrophic–heterotrophic balance. Elevated bed shear-stress velocity promotes the movement of bed sediments and effectively reduces  $GPP$  about two times more than the corresponding  $R$  (Cronin *et al.*, 2007).

## CONCLUSION

The *in situ* measurement of DO concentration has been used for the estimation of metabolism of flowing water communities. The estimation methods employ one-station and two-station estimators. The methods rely on the estimation of spatial and temporal variabilities of DO in the water. We conducted field measurements in Minnehaha Creek, MN, to quantify the spatial and temporal variabilities of DO concentrations and consequently evaluate the estimates of stream metabolism quantified by NP. Two alternative estimation methods of stream metabolism (Bott, 2006; Reichert *et al.*, 2009) provided similar estimates of NP with  $0.65 > k_a T_a > 0.17$  within the studied reach. The fundamental assumption using two-station methods is the existence of a characteristic velocity with which successive parcels of water are advected between the measuring stations. Our DO measurements along the creek suggest that the concept of plug flow transport of designated parcels of water with associated DO concentrations should be revisited because DO concentrations were significantly autocorrelated over an average distance of 10 m along the studied reach.

The dimensionless analysis of DO mass balance revealed the dominance of photosynthesis over respiration, advection, aeration, and transport by dispersion along the studied reach over the days of measurement during the summer growth period. The autotrophic–heterotrophic balance, quantified by *GPP* to *R* ratio, scaled directly to stream width to depth ratio and scaled inversely to stream bed resistance conditions.

## ACKNOWLEDGEMENT

This work was supported by the National Center for Earth-surface Dynamics (NCED), a Science and Technology Center funded by the Office of Integrative Activities of the National Science Foundation (under agreement EAR-0120914). The authors are grateful for valuable comments from the reviewers which significantly improved this manuscript.

## REFERENCES

- Barnes EA, Power ME, Fofoula-Georgiou E, Hondzo M, Dietrich WE. 2007. Upscaling river biomass using dimensional analysis and hydrogeomorphic scaling. *Geophysical Research Letters* **34**: L24S26. DOI: 10.1029/2007GL031931.
- Bernot JM, Sobta DJ, Hall RO, Mulholland PJ, Dodds WK, Webster JR, Tank JL, Ashkenas LR, Cooper LW, Dahm CN, Gregory SV, Grimm NB, Hamilton SK, Johnson SL, McDowell WH, Meyer JL, Peterson B, Poole GC, Valett HM, Arango C, Beaulieu JJ, Burgin AJ, Crenshaw C, Helton AM, Johnson L, Merriam J, Neiderlehner BR, O'Brien JM, Potter JD, Sheibley RW, Thomas SM, Wilson K. 2010. Inter-regional comparison of land-use effects on stream metabolism. *Freshwater Biology* **55**: 1874–1890. DOI: 10.1111/j.1365-2427.2010.02422.x
- Bewley GP, Chang K, Bodenschatz E. 2012. On integral length scale in anisotropic turbulence. *Physics of Fluids* **24**(061702): 1–7.
- Biggs BJF, Smith RA, Duncan M. 1999. Velocity and sediment disturbance of periphyton in headwater streams: biomass and metabolism. *Journal of the North American Benthological Society* **18**: 222–241.
- Biggs BJF, Nikora VI, Snelder TH. 2005. Linking scales of flow variability to lotic ecosystem structure and function. *River Research and Applications* **21**: 283–298.
- Bott TL. 2006. Primary productivity and community respiration. In *Methods in Stream Ecology* Lamberti FRHaGA (ed). Academic Press: San Diego, CA; 663–689.
- Bott TL, Newbold JD, Arscott DB. 2006. Ecosystem metabolism in Piedmont streams: reach geomorphology modulates the influence of riparian vegetation. *Ecosystems* **9**: 398–421. DOI: 10.1007/s10021-005-0086-6
- Chapra SC, Di Torro DM. 1991. Delta method for estimating primary production, respiration, and reaeration in streams. *Journal of Environmental Engineering* **117**: 640–655.
- Chu CR, Jirka GH. 2003. Wind and stream flow induced reaeration. *Journal of Environmental Engineering* **129**: 1129–1136.
- Cronin G, McCutchan, Jr. GH, Pitlick J, Lewis, Jr. WM. 2007. Use of shields stress to reconstruct and forecast changes in river metabolism. *Freshwater Biology* **52**: 1587–1601. DOI: 10.1111/j.1365-2427.2007.01790.x
- Demars BOL, Manson JR, Olafson JS, Gislason GM, Gudmundsdottir R, Woodward G, Reiss J, Pichler DE, Rasmussen JJ, Friberg N. 2011. Temperature and the metabolic balance of streams. *Freshwater Biology* **56**: 1106–1121. DOI: 10.1111/j.1365-2427.2010.0554.x.
- Dodds WK, Cole JJ. 2007. Expanding the concept of trophic state in aquatic ecosystems: It's not just the autotrophs. *Aquatic Sciences* **69**: 427–439.
- Erdman JB. 1979. Systematic diurnal curve analysis. *Journal Water Pollution Control Federation* **51**: 78–86.
- Ettema CH, Wardle DA. 2002. Spatial soil ecology. *Trends in Ecology & Evolution* **17**: 177–183.
- Fellows CS, Valett HM, Dahm CN, Mulholland PJ, Thomas SA. 2006. Coupling nutrient uptake and energy flow in headwater streams. *Ecosystems* **9**: 788–804. DOI: 10.1007/s10021-006-0005-5.
- Finlay JC. 2011. Stream size and human influences on ecosystem production in river networks. *Ecosphere* **2**(8): DOI: 10.1890/ES11-00071.1
- Finlay JC, Hood JM, Limm MP, Power ME, Schade JD, Wulder JR. 2011. Light-mediated thresholds in stream water nutrient composition in a river network. *Ecology* **92**: 140–150. DOI: 10.1890/09-2243.1
- Fischer HB. 1975. Simple method for predicting dispersion in streams. *Journal of Environmental Engineering* **101**: 453–455.
- Fisher SG, Sponseller RA, Heffernan JB. 2004. Horizons in stream biogeochemistry: flowpaths to progress. *Ecology* **85**: 2369–2379.
- Hall CAS. 1972. Migration and metabolism in a temperate stream ecosystem. *Ecology* **53**: 585–604.
- Hassan YA, Gutierrez-Torres CC, Jimenez-Bernal JA. 2005. Temporal correlation modification by microbubbles injection in a channel flow. *International Communications in Heat and Mass Transfer* **32**: 1009–1015.
- Hornberger GM, Kelly MG. 1975. Atmospheric reaeration in a river using productivity analysis. *Journal of Environmental Engineering* **101**: 729–739.
- Hornberger GM, Kelly MG, Cosby BJ. 1977. Evaluating eutrophication potential from river community productivity. *Water Research* **11**: 65–69.
- Hunt RJ, Jardine TD, Hamilton SK, Bunn SE. 2012. Temporal and spatial variation in ecosystem metabolism and food web carbon transfer in a wet-dry tropical river. *Freshwater Biology* **57**: 435–450. DOI:10.1111/j.1365-2427.2011.02708.x.
- Jain SK, Jha R. 2005. Comparing the stream re-aeration coefficient estimated from ANN and empirical models. *Hydrological Sciences* **50**: 1037–1052.
- Knapp CW, Dodds WK, Wilson KC, O'Brien JM, Graham DW. 2009. Spatial heterogeneity of denitrification genes in a highly homogenous urban stream. *Environmental Science and Technology* **43**: 4273–4279.
- Kundu P. 1990. *Fluid Mechanics*. Academic Press: San Diego, CA. ISBN: 0124287700
- Loperfido JV, Just CL, Schnoor JL. 2009. High-frequency diel dissolved oxygen stream data modeled for variable temperature and scale. *Journal of Environmental Engineering* **135**(2): 1250–1256.
- McClain ME, Boyer EW, Dent CL, Gergel SE, Grimm NB, Groffman PM, Hart SC, Harvey JW, Johnston CA, Mayorga E, McDowell WH, Pinay G. 2003. Biogeochemical hot spots and hot moments at the interface of terrestrial and aquatic ecosystems. *Ecosystems* **6**: 301–312.

- McCutchan JH, Lewis, Jr. WM. 2006. Groundwater flux and open-channel estimation of stream metabolism: response to Hall and Tank. *Limnology and Oceanography Methods* **4**: 213–215.
- McTammany ME, Webster JR, Benfield EF, Neatrour MA. 2003. Logitudinal patterns of metabolism in a southern Appalachian river. *Journal of the North American Benthological Society* **22**: 359–370.
- Mulholland PJ, Fellows CS, Tank JL, Webster JR, Hamilton SK, Marti E, Ashkenas L, Bowden WB, Dodds WK, Dowell WH, Paul MJ, Peterson BJ. 2001. Inter-biome comparison of factors controlling stream metabolism. *Freshwater Biology* **46**: 1503–1517.
- O'Connor DJ, Dobbins WE. 1958. Mechanisms of reaeration in natural streams. *Transactions ASCE* **123**: 641–684.
- O'Connor LB, Hondzo M. 2007. Enhancement and inhibition of denitrification by fluid-flow and dissolved oxygen flux to stream sediments. *Environmental Science and Technology* **42**: 119–125. DOI: 10.1021/es071173s.
- O'Connor LB, Hondzo M, Dobraca D, LaPara T, Finlay J, Brezonik PL. 2006. Quantity-activity relationship of denitrifying bacteria and environmental scaling in streams of forested watershed. *Journal of Geophysical Research- Biogeosciences* **111**(G04014): 1–13.
- Odum HT. 1956. Primary production in flowing waters. *Limnology and Oceanography* **1**: 102–117.
- Podlubny I. 1999. Fractional Differential Equations: An Introduction to Fractional Derivatives, Fractional Differential Equations, to Methods of Their Solution and Some of Their Applications. Academic Press: San Diego, CA.
- Reichert P, Uehlinger U, Acuña V. 2009. Estimating stream metabolism from oxygen concentrations: effect of spatial heterogeneity. *Journal of Geophysical Research* **114**: G03016. DOI 10.1029/2008JG000917.
- Roberts BJ, Mulholland PJ, Hill WR. 2007. Multiple scales of temporal variability in ecosystem metabolism rates: results from 2 years of continuous monitoring in a forested headwater stream. *Ecosystems* **10**: 588–606.
- Uehlinger U, König C, Reichert P. 2000. Variability of photosynthesis-irradiance curves and ecosystem respiration in a small river. *Freshwater Biology* **44**: 493–507.
- Vannote RL, Minshall GW, Cummins KW, Sedell JR, Cushing CE. 1980. The river continuum concept. *Canadian Journal of Fisheries and Aquatic Sciences* **37**: 130–137.
- Wang H, Hondzo M, Xu C, Poole V, Spacie A. 2003. Dissolved oxygen dynamics of streams draining an urbanized and agricultural catchment. *Ecological Modelling* **160**: 145–161.
- Warnaars T, Hondzo M, Power EM. 2007. Abiotic controls on periphyton accrual and metabolism in streams: scaling by dimensionless numbers. *Water Resources Research* **43**: W08425. DOI: 10.1029/2006WR005002.
- Young RG, Huryn AD. 1998. Comment: improvements to the diurnal upstream-downstream dissolved oxygen change technique for determining whole-stream metabolism in small streams. *Canadian Journal of Fisheries and Aquatic Sciences* **55**: 1784–1785.
- Zell C, Hubbart JA. 2012. An evaluation of light intensity functions for determination of shaded reference stream metabolism. *Journal of Environmental Management* **97**: 69–77.